

# Anomalous photoluminescence behavior from amorphous Ge quantum dots produced by buffer-layer-assisted growth

A. S. Bhatti

*Department of Materials Science & Engineering, University of Illinois at Urbana-Champaign, Illinois 61801 and Center for Micro and Nano Devices, Department of Physics, COMSATS Institute of Information Technology, Jauhar Campus, Islamabad 44000, Pakistan*

V. N. Antonov

*Department of Physics, University of Illinois at Urbana-Champaign, Illinois 61801*

P. Swaminathan, J. S. Palmer, and J. H. Weaver<sup>a)</sup>

*Department of Materials Science & Engineering, University of Illinois at Urbana-Champaign, Illinois 61801*

(Received 19 September 2006; accepted 28 November 2006; published online 2 January 2007)

The authors present photoluminescence results from amorphous Ge quantum dots formed using buffer-layer-assisted growth. Their sizes, shapes, and densities were controlled by varying the thickness of the Xe buffer layer, with sizes varying from 2 to 8 nm. A relatively weak signal was observed at  $\sim 3$  K at  $\sim 0.91$  eV that was independent of size and was insensitive to laser intensity. Its temperature-dependent magnitude showed a Berthelot-type behavior that they associate with hopping of carriers between radiative tail states and shallow nonradiative states. These findings are similar to those from porous semiconductors. © 2007 American Institute of Physics.

[DOI: 10.1063/1.2426892]

Recent theoretical studies have shown that the poor light emitting properties of Si and Ge can be improved by making use of low-dimensional Si/Ge structures.<sup>1</sup> Accordingly, Ge quantum dots have attracted considerable attention with the hope of integrating electronic and optoelectronic devices on the same platform.<sup>2-4</sup> Studies of “dry” synthesis via physical vapor deposition have shown that a Ge wetting layer first forms on Si(100), and that the 4.2% lattice match then favors the development of dots.<sup>5-8</sup> Unfortunately, the wetting layer also couples adjacent dots electronically, reducing the quantum confinement and providing an escape channel for thermally excited carriers.

A very simple technique termed buffer-layer-assisted growth (BLAG) makes it possible to produce three dimensional nanostructures of a wide variety of materials.<sup>9-11</sup> It involves vapor deposition of the material of choice onto condensed rare gas buffer layers that isolate the forming structures from the substrate. Subsequent warm-up delivers them to the pristine substrate. Previous structural studies have shown that Ge dots formed in this way are amorphous, and cross-sectional transmission electron microscopy images demonstrate an abrupt interface between them and Si, i.e., quantum dots without a wetting layer.<sup>12,13</sup>

In this letter, we discuss photoluminescence (PL) studies of Ge dots grown by BLAG on oxidized Si(100) and encapsulated by CaF<sub>2</sub>. By tuning the buffer layer thickness, we were able to vary the dot densities and sizes, producing both compact and elongated structures. Power- and temperature-dependent PL spectroscopies were used to determine the origin of the emission band. We show that the integrated intensity exhibits anomalous behavior with temperature known as Berthelot, which is explained using a model that is analogous to one developed for porous semiconductors. In particular, it reflects the presence of a large number of shallow defect (nonradiative) states close in energy to radiative states in the

band tails.<sup>14-16</sup> These nonradiative shallow states not only offer a route for depleting carriers but also act as source for populating radiative states, introducing a peak in PL intensities as a function of temperature.

The samples were grown in an ultrahigh vacuum system, as described in detail in Ref. 10. Here, 1 Å of Ge was deposited on Xe buffers of 4, 10, 20, and 30 ML (monolayer) thickness. PL spectroscopy was performed at  $\sim 3$  K in a liquid-He-bath optical cryostat. Excitation was done with an Ar<sup>+</sup> laser using the 514 nm (2.41 eV) line, and the emitted light was collected by a single stage monochromator and detected by a liquid-N<sub>2</sub>-cooled Ge detector. All spectra were corrected for the system response. The laser excitation intensities were varied from 100 to 700 W cm<sup>-2</sup>, and the temperature was controlled with a heater on the cold head.

The atomic force microscopy (AFM) images of Fig. 1 show Ge dots on oxidized Si with no capping layer for the buffer thicknesses indicated. Their density followed a power law dependence on buffer thickness, as expected for diffusion limited cluster aggregation,<sup>10</sup> dropping from  $1.6 \times 10^{11}$  to  $4.6 \times 10^9$  cm<sup>-2</sup> for Xe buffers from 10 to 40 ML thick. The insets show that the height distributions are quite uniform for thin buffers but that the distribution shifts to larger sizes and broadens asymmetrically for thicker buffers. The average radius increases from  $1.5 \pm 0.5$  to  $8.0 \pm 2.0$  nm and from 4 to 40 ML buffer thicknesses, much smaller than those grown by conventional methods.

Following the model of Estes and Moddel,<sup>17</sup> Fig. 2 depicts photogenerated carriers created in the conduction and valence bands that thermalize to the lowest energy tail states. Radiative (R) recombination involves transitions between tail states while nonradiative (NR) recombination involves transitions to optically inactive defect centers that lie near the midgap. We assume that the density of tail states is independent of dot size since it is determined primarily by nearest neighbors.<sup>17</sup>

<sup>a)</sup>Electronic mail: jhweaver@uiuc.edu

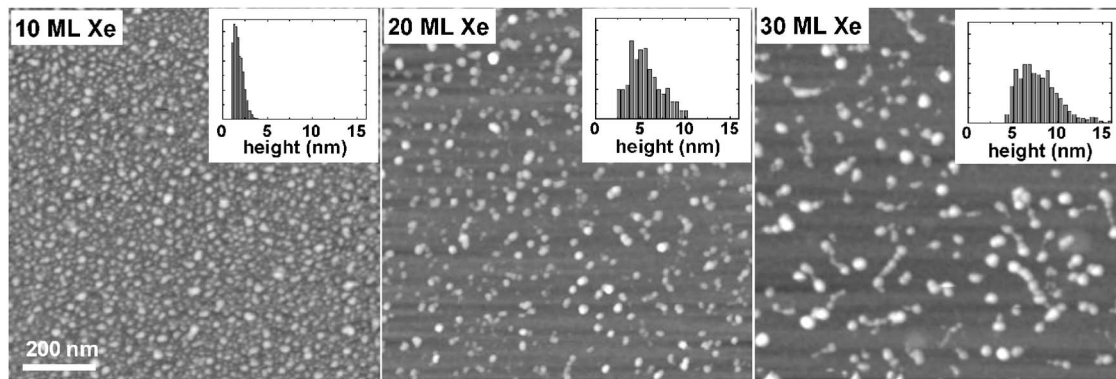


FIG. 1. AFM images of Ge quantum dots obtained by depositing 1 Å of Ge on Xe buffers of 10–30 ML thickness. The insets show that the size distributions broaden with increasing buffer thickness.

The upper part of Fig. 3 shows a representative PL spectrum of 1 Å Ge grown on a 4 ML thick Xe buffer layer on oxidized Si(100) and capped with CaF<sub>2</sub> before air exposure. The box draws attention to the feature that arises from Ge; the others are signatures of Si. This band around 0.91 eV persists in spectra from samples grown with thicker buffers, as shown in the lower part of Fig. 3. It does not shift in energy as the dots grow in size but it does broaden asymmetrically with increased dot size. The absence of a shift is an indication that tail states are responsible for the PL signal.

In crystalline nanostructures, quantum confinement leads to an increase in the band gap with decreasing size, which results in blueshift of the PL peak. For amorphous nanostructures with recombination involving localized tail states, one must consider spatial carrier confinement.<sup>17</sup> A capture radius defines a volume that contains both radiative and nonradiative states that are accessible for photogenerated carriers. If this volume has (does not have) a dangling bond, then there will be nonradiative (radiative) recombination. A shift in the PL band will be observed with increasing dot size if the capture radius remains larger than the dot size. Assuming a lower limit of dangling bond density of 10<sup>20</sup> cm<sup>-3</sup>,<sup>18</sup> the capture radius of the Ge dots grown by BLAG is a few angstroms. Because this capture radius is less than the size of the dots, the position of the PL peak is insensitive to particle size.

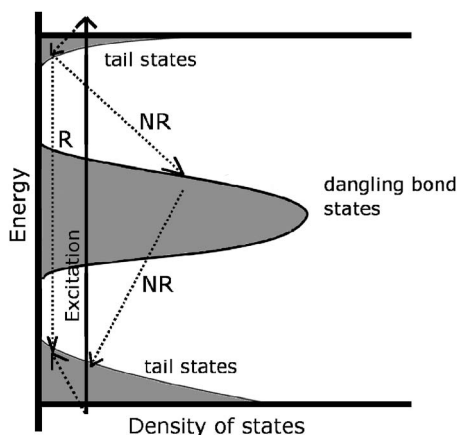


FIG. 2. Simplified depiction of the distribution of states for an amorphous Ge dot showing localized tail states extending beyond the limits of the nominal conduction and valence bands, together with dangling bond states of intermediate energies. Excited carriers can decay radiatively (R) from tail states or nonradiatively (NR) through dangling bond states.

Power dependent PL measurements showed a sublinear dependence of intensity (slope less than 0.1 mW<sup>-1</sup> for all samples) with no shift at higher excitation intensities. This indicates a dominant role for defect states contributing in nonradiative recombination. While we cannot be quantitative, the density of radiative tail states must be very small compared with defect states to account for the sublinear behavior.

Figure 4(a) shows representative PL spectra for 1 Å Ge grown on 10 ML of Xe taken with an excitation density of 200±10 W cm<sup>-2</sup> at various temperatures. The 0.91 eV feature is sharp and asymmetric at 3 K, and it broadens with temperature and disappears above ~90 K. Between 3 and 90 K, there is a redshift of only 2 meV, compared to an expected shift of 10 meV for free excitonic recombination.<sup>19</sup> The symbols in Fig. 4(b) summarize the total integrated intensity as a function of reciprocal temperature after background subtraction.

The behavior of Fig. 4(b) can be understood qualitatively in terms of excited electrons and holes that relax to the conduction and valence band tail states which can be radiative and nonradiative. At low temperatures ( $T \sim 3$  K), where electron and hole mobilities can be neglected, radiative re-

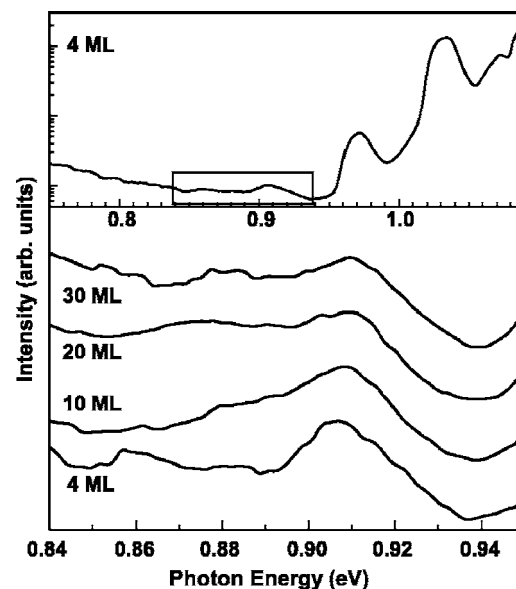


FIG. 3. Normalized PL spectra from Ge dots grown on 4, 10, 20, and 30 ML of Xe taken at ~3 K. The upper part of the figure shows the full PL spectrum with the box drawing attention to the region of interest.

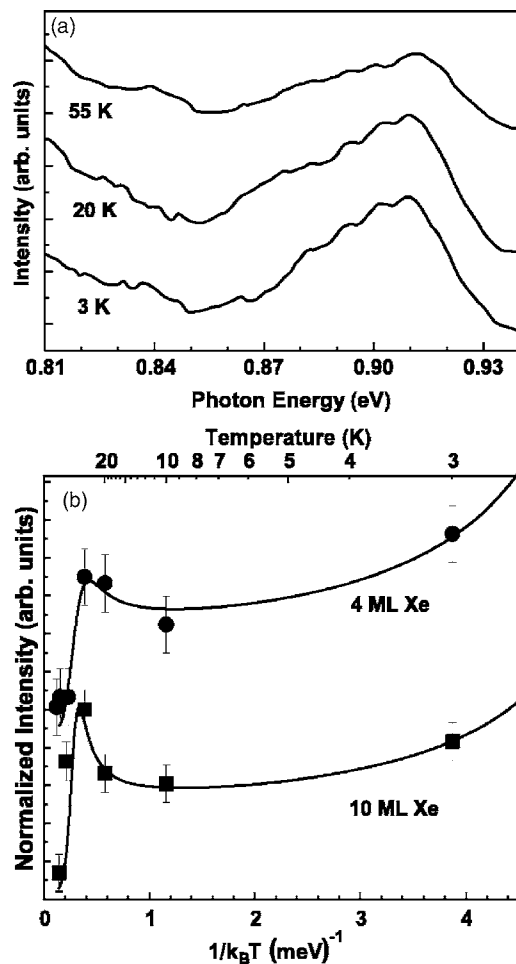


FIG. 4. (a) PL spectra at various temperatures of Ge dots formed on 10 ML Xe. (b) Integrated PL intensity for samples grown with buffer thicknesses of 4 and 10 ML Xe to determine the Berthelot temperature and the activation energy as a function of  $(k_B T)^{-1}$ . The symbols are the experimental points while the curves are fits of Eq. (1).

combination is at its maximum as there is no thermal diffusion of carriers to shallow or deep defects. As the temperature increases, carrier hopping is activated from the radiative tail states of Fig. 2, resulting in a decrease in PL as the states are depleted. At higher temperature,  $\sim 30$  K, it is possible to excite carriers from nonradiative tail states into the radiative tail states. This process has an anomalous Berthelot-type behavior, and it is responsible for the increase in intensity in the region of 20–40 K in Fig. 4(b). It is a typical case of two quantum wells with varying heights and overlapping wave functions; with a small increase in temperature, the sink becomes the source. At about 40 K, carriers can escape to deep defect states, and PL is quenched.

The temperature-dependent behavior can be quantified by assuming that the PL decay rate depends on a radiation rate, a hopping rate for the Berthelot behavior, and a carrier escape rate. The radiation rate and carrier escape rate to the deep levels follow Arrhenius temperature dependencies with activation energies  $E_r$  and  $E_{\text{esc}}$ . The hopping rate has an anomalous Berthelot temperature dependence with characteristic temperature  $T_B$  and energy  $E_B$ . The energies  $E_r$ ,  $E_{\text{esc}}$ , and  $E_B$  determine the rates of the R and NR processes, depicted in Fig. 2 and the hopping between tail states (radiative

and nonradiative shallow states), respectively. Combining these three processes yields the total integrated intensity variation with temperature,

$$I(T)/I_0 = [1 + \nu_1^* \exp((k_B T/E_B) + (E_r/k_B T)) + \nu_2^* \exp((E_r - E_{\text{esc}})/k_B T)]^{-1}, \quad (1)$$

where  $I_0$  is the normalization parameter and  $\nu_1^*$  and  $\nu_2^*$  are the effective frequencies. The solid lines in Fig. 4(b) are fits with energies and frequencies as free parameters.<sup>14</sup> The fit gives  $T_B$ 's of  $23 \pm 7$  and  $27 \pm 4$  K for the 4 and 10 ML samples, in the theoretically predicted range for particles of size of 1–10 nm.<sup>14</sup>  $E_{\text{esc}} = 16 \pm 4$  and  $25 \pm 2$  meV for the 4 and 10 ML samples while  $E_r = k_B T_r$  is small, as expected,  $\sim 0.3$  meV for both samples.

We have measured PL of amorphous Ge quantum dots with varied sizes and densities grown by buffer-layer-assisted growth. The PL signal originates from localized band tail states and shows a strong Berthelot temperature behavior analogous to PL from porous semiconductors. The presence of such a Berthelot behavior in our *a*-Ge quantum dots is primarily due to the presence of a large number of shallow nonradiative tail states energetically near the localized radiative tail states.

This work was supported by a NSF International Program and the U.S. Department of Energy, Division of Materials Sciences under Grant No. DEFG02-01ER45944. One of the authors (A.S.B.) acknowledges support from the Abdus Salam International Center for Theoretical Physics. The measurements were done in the Laser Laboratory of the Center for Microanalysis of Materials of the Frederick Seitz Materials Research Laboratory, which is partially supported by the U.S. Department of Energy under Grant No. DEFG02-91-ER45439. The authors thank J. A. N. T. Soares for expert assistance.

<sup>1</sup>F. A. Reboredo and Alex Zunger, Phys. Rev. B **62**, R2275 (2000).

<sup>2</sup>M. Kastner and B. Voigtlander, Phys. Rev. Lett. **82**, 2745 (1999).

<sup>3</sup>M. W. Dashiell, U. Denker, and O. G. Schmidt, Appl. Phys. Lett. **79**, 2261 (2001).

<sup>4</sup>O. G. Schmidt, C. Lange, and K. Eberl, Appl. Phys. Lett. **75**, 1905 (1999).

<sup>5</sup>D. J. Eaglesham and M. Cerullo, Phys. Rev. Lett. **64**, 1943 (1990).

<sup>6</sup>G. Medeiros-Ribeiro, A. M. Bratkovski, T. I. Kamins, D. A. A. Ohlberg, and R. S. Williams, Science **279**, 353 (1998).

<sup>7</sup>G. Jin, J. L. Liu, S. G. Thomas, Y. H. Lou, K. L. Wang, and B.-Y. Nguyen, Appl. Phys. Lett. **75**, 2752 (1999).

<sup>8</sup>Vinh Le Thanh, P. Boucaud, D. Debarre, Y. Zheng, D. Bouchier, and J.-M. Lourtioz, Phys. Rev. B **58**, 13115 (1998).

<sup>9</sup>J. H. Weaver and G. D. Waddill, Science **251**, 1444 (1991).

<sup>10</sup>V. N. Antonov, J. S. Palmer, A. S. Bhatti, and J. H. Weaver, Phys. Rev. B **68**, 205418 (2003).

<sup>11</sup>V. N. Antonov, P. Swaminathan, J. A. N. T. Soares, J. S. Palmer, and J. H. Weaver, Appl. Phys. Lett. **88**, 121906 (2006).

<sup>12</sup>K. Yoo, A.-P. Li, Z. Y. Zhang, H. H. Weitering, F. Flack, M. G. Lagally, and J. F. Wendelken, Surf. Sci. **546**, L803 (2003).

<sup>13</sup>A. P. Li, F. Flack, M. G. Lagally, M. F. Chisholm, K. Yoo, Z. Y. Zhang, H. H. Weitering, and J. F. Wendelken, Phys. Rev. B **69**, 245310 (2004).

<sup>14</sup>M. Kapoor, V. A. Singh, and G. K. Johri, Phys. Rev. B **61**, 1941 (2000).

<sup>15</sup>H. Rinnert and M. Vergnat, Physica E (Amsterdam) **16**, 382 (2003).

<sup>16</sup>J. L. Liu, Y. S. Tang, K. L. Wang, T. Radetic, and R. Gronsky, Appl. Phys. Lett. **74**, 1863 (1999).

<sup>17</sup>M. J. Estes and G. Moddel, Phys. Rev. B **54**, 14633 (1996).

<sup>18</sup>S. C. Agarwal, Phys. Rev. B **7**, 685 (1973).

<sup>19</sup>Y. P. Varshni, Physica (Amsterdam) **34**, 149 (1967).